

DOI: 10.1002/asia.201301106

Highly Active, Low-Valence Molybdenum- and Tungsten-Amide Catalysts for Bifunctional Imine-Hydrogenation Reactions

Subrata Chakraborty, Olivier Blacque, Thomas Fox, and Heinz Berke*^[a]

Abstract: The reactions of $[M(\text{NO})(\text{CO})_4(\text{ClAlCl}_3)]$ ($M = \text{Mo}, \text{W}$) with $(i\text{Pr}_2\text{PCH}_2\text{CH}_2)_2\text{NH}$, (PN^HP) at 90°C afforded $[M(\text{NO})(\text{CO})(\text{PN}^H\text{P})\text{Cl}]$ complexes ($M = \text{Mo}, \mathbf{1a}$; $\text{W}, \mathbf{1b}$). The treatment of compound $\mathbf{1a}$ with $\text{KO}t\text{Bu}$ as a base at room temperature yielded the alkoxide complex $[M(\text{NO})(\text{CO})(\text{PN}^H\text{P})(\text{O}t\text{Bu})]$ ($\mathbf{2a}$). In contrast, with the amide base $\text{Na}[\text{N}(\text{SiMe}_3)_2]$, the PN^HP ligand moieties in compounds $\mathbf{1a}$ and $\mathbf{1b}$ could be deprotonated at room temperature, thereby inducing dehydrochlorination into amido complexes $[M(\text{NO})(\text{CO})(\text{PNP})]$ ($M = \text{Mo}, \mathbf{3a}$; $\text{W}, \mathbf{3b}$; $\text{PNP} = (i\text{Pr}_2\text{PCH}_2\text{CH}_2)_2\text{N}$). Compounds $\mathbf{3a}$ and $\mathbf{3b}$ have pseudo-trigonal-bipyramidal geometries, in which the amido nitrogen atom is in the equatorial plane. At room temperature, compounds $\mathbf{3a}$

and $\mathbf{3b}$ were capable of adding dihydrogen, with heterolytic splitting, thereby forming pairs of isomeric amine-hydride complexes $[\text{Mo}(\text{NO})(\text{CO})\text{H}(\text{PN}^H\text{P})]$ ($\mathbf{4a(cis)}$ and $\mathbf{4a(trans)}$) and $[\text{W}(\text{NO})(\text{CO})\text{H}(\text{PN}^H\text{P})]$ ($\mathbf{4b(cis)}$ and $\mathbf{4b(trans)}$); *cis* and *trans* correspond to the position of the H and NO groups). H_2 approaches the $\text{Mo/W}=\text{N}$ bond in compounds $\mathbf{3a,b}$ from either the CO-ligand side or from the NO-ligand side. Compounds $\mathbf{4a(cis)}$ and $\mathbf{4a(trans)}$ were only found to be stable under a H_2 atmosphere and could not be isolated. At 140°C and 60 bar H_2 , compounds $\mathbf{3a}$ and $\mathbf{3b}$ catalyzed the hydrogenation of imines,

thereby showing maximum turnover frequencies (TOFs) of 2912 and 1120 h^{-1} , respectively, for the hydrogenation of *N*-(4-methoxybenzylidene)aniline. A Hammett plot for various *para*-substituted imines revealed linear correlations with a negative slope of -3.69 for *para* substitution on the benzylidene side and a positive slope of 0.68 for *para* substitution on the aniline side. Kinetics analysis revealed the initial rate of the hydrogenation reactions to be first order in $c(\text{cat.})$ and zeroth order in $c(\text{imine})$. Deuterium kinetic isotope effect (DKIE) experiments furnished a low $k_{\text{H}}/k_{\text{D}}$ value (1.28), which supported a Noyori-type metal–ligand bifunctional mechanism with H_2 addition as the rate-limiting step.

Keywords: amides · hydrogenation · imines · molybdenum · tungsten

Introduction

The catalytic hydrogenation of polar unsaturated functional groups has been widely applied in industry and in academia. These reactions mainly proceed along Wilkinson and Osborn hydrogenation mechanisms,^[1] which involve the following key steps: 1) Coordination of the unsaturated substrate onto a vacant metal center; 2) *cis*-insertion of the substrate into a metal–hydride bond; 3) homolytic splitting of H_2 through oxidative addition to the metal center; and 4) reductive elimination of a C–H bond to afford the saturated product. Alternatively, the hydrogenation reactions may occur with a “bifunctional” metal–ligand system with more or less simultaneous heteropolar H-atom transfer onto unsaturated substrates.^[2,3] The preceding heterolytic splitting of

H_2 creates protic and hydridic moieties, followed by stepwise or concerted H^+ and H^- transfer onto the unsaturated organic substrates. These reactions are also denoted as protonic-hydridic catalysis or ionic hydrogenation, depending on the character of the H-atom transfer.^[4,5] Recently, bifunctional homogeneous catalysis has attracted increasing attention, triggered by the elegant initial work by the groups of Noyori,^[6] Ikariya,^[7] Milstein,^[8] Shvo,^[9a,d] and Casey.^[9b,c] In these reactions, the heterolytic cleavage of H_2 occurs across a metal=O/N-ligand double bond. In recent years, transition-metal hydrides that contain the protic PN^HP ligand ($\text{PN}^H\text{P} = (i\text{Pr}_2\text{PCH}_2\text{CH}_2)_2\text{NH}$) have been found to be suitable for various types of bifunctional H_2 transformations, such as hydrogenation,^[10] transfer hydrogenation,^[11] and dehydrogenation reactions.^[12,13] However, traditionally, the catalysts that were used in these reactions were mostly based on the platinum-group metals Ru, Rh, and Ir,^[14] which have to be recycled in larger-scale transformations. Therefore, efforts to replace these metals with non-precious and, importantly, less-toxic metals (“cheap metals for noble tasks”)^[15] is an appealing challenge. Thus, in recent years, iron catalysis has received significant attention.^[16] Molybdenum and tungsten catalysis would also largely satisfy these requirements and offer valuable alternatives to platinum-group

[a] Dr. S. Chakraborty, Dr. O. Blacque, Dr. T. Fox, Prof. H. Berke
Institute of Inorganic Chemistry
University of Zurich
Winterthurerstrasse 190
CH-8057 Zurich (Switzerland)
E-mail: hberke@aci.uzh.ch

Supporting information for this article is available on the WWW under <http://dx.doi.org/10.1002/asia.201301106>.

metals, owing to their low cost and environmentally benign nature. However, the organometallic chemistry of molybdenum and tungsten for their application in effective homogeneous hydrogenation reactions remains insufficiently explored. The initial work of Bullock et al.^[17] on ionic hydrogenation reactions of ketones and our work^[18] on the hydrogenation of imines catalyzed by molybdenum and tungsten systems seem to be promising cases for catalyst-tuning efforts.

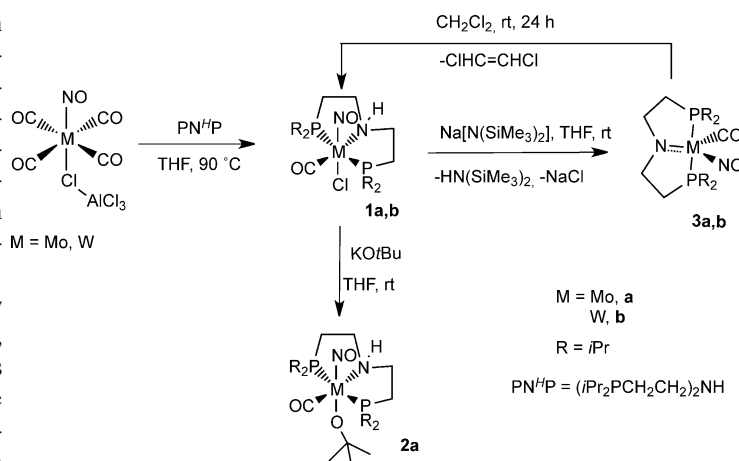
Replacing expensive and toxic platinum-group metals by complexes with middle-transition-metal elements rhenium, molybdenum, and tungsten has been a long-standing focus of our research group. In fact, we recently reported^[19] the tuning of rhenium-nitrosyl-based catalysts to afford excellent performance for the hydrogenation of olefins (with comparable activities to precious-metal catalysts), as well as other hydrogen-related reactions, such as hydrosilylation,^[20] dehydrogenative silylation,^[21] and dehydrogenative amino-borane-coupling reactions.^[22]

Because, in bifunctional catalysis, simultaneous transfer of the proton and the hydride is perceived to happen in the secondary coordination sphere, one might, in principal, anticipate less influence of the metal center, which, consequently, would make many transition metals suited for the given task. Herein, we sought to confirm the ability of appropriately substituted molybdenum and tungsten centers in low oxidation states to interact with H₂ and then to test these catalysts in hydrogenation reactions.

Results and Discussion

Preparation of Amino and Amido Complexes 1a–3b

New pentacoordinate Mo⁰- and W⁰-amide complexes [M(NO)(CO)(PNP)] (M=Mo, **3a**; W, **3b**; PNP = (iPr₂PCH₂CH₂)₂N) were synthesized by ligand-substitution reactions. Thus, the reaction of precursor complexes [Mo(NO)(CO)₄(ClAlCl₃)] and [W(NO)(CO)₄(ClAlCl₃)] with (iPr₂PCH₂CH₂)₂NH in THF at 90 °C resulted in the formation of [Mo(NO)(CO)(PN^HP)Cl] (**1a**) and [W(NO)(CO)(PN^HP)Cl] (**1b**, Scheme 1), which were isolated in 74% and 78% yield, respectively. The IR spectra of compounds **1a** and **1b** exhibited strong ν(CO) absorptions at 1912 and 1894 cm⁻¹, respectively. Single-crystal X-ray diffraction analysis^[33] of compounds **1a** and **1b** (see the Supporting Information) showed that the metal centers possessed distorted octahedral geometries. The nitrosyl groups were positioned *trans* to the chloride ligand in both cases. The existence of *cis* and *trans* isomers of the nitrosyl groups with respect to the position of the amine proton (N–H) in compounds **1a** or **1b** was supported by the observation of two signals in the ³¹P{¹H} NMR spectra. Attempts to separate the isomers of compounds **1a** and **1b** failed, even by column chromatography at low temperatures. The isomers showed similar deprotonation behaviors and, therefore, could be used as a mixture in the subsequent deprotonation reactions.



Scheme 1. Preparation of the amino and amido complexes.

The application of KOtBu to the reaction with compound **1a** at room temperature led to chloride substitution, thereby forming alkoxide complex [Mo(NO)(CO)(PN^HP)(OtBu)] (**2a**, Scheme 1). The ³¹P{¹H} NMR spectrum of compound **2a** only showed a single resonance at δ = 52 ppm, which provided evidence for the chemical equivalence of the phosphorus atoms and the absence of isomers. A strong IR band at 1883 cm⁻¹ indicated the presence of a CO group. X-ray diffraction analysis^[33] of compound **2a** (see the Supporting Information, Figure S3) revealed a pseudo-octahedral geometry around the metal center.

Reactions of compounds **1a** and **1b** with the comparatively strong and sterically hindered amide base Na[N(SiMe₃)₂] led to dehydrochlorination with deprotonation of the N–H moieties to form the highly air-sensitive and reactive 16e⁻ complexes [M(NO)(CO)(PNP)] (M=Mo, **3a**; W, **3b**) in 57% and 54% yield, respectively (Scheme 1). IR bands at 1893 (**3a**) and at 1871 cm⁻¹ (**3b**) were assigned to the carbonyl ligands. The ³¹P{¹H} NMR spectra of compounds **3a** and **3b** showed unique signals at δ = 82 and 81 ppm, thus suggesting chemical equivalence of the phosphorus atoms and the absence of isomers. These complexes were quite soluble in benzene, toluene, and THF. Presumably owing to a relatively high degree of unsaturation of the metal centers, the complexes reacted in CH₂Cl₂ to gradually form chloride complexes **1a,b**, although the formation of supposed by-product 1,2-dichloroethene was not detected in the ¹H NMR spectra. The formation of compounds **1a,b** was supported by X-ray diffraction of compound **1a** (obtained from the reaction of compound **3a** with CH₂Cl₂) and by ¹H and ³¹P NMR spectroscopy; moreover, the addition of Na[N(SiMe₃)₂] caused the regeneration of amido complexes **3a,b**. Deep-red single crystals suitable for X-ray diffraction were obtained for compounds **3a** and **3b** from concentrated solutions in pentane at –30 °C.

Importantly, coordinatively unsaturated neutral amides **3a** and **3b** are the first structurally characterized pentacoordinate d⁶ Mo- and W-amido complexes.^[23] The structures of compounds **3a** and **3b** are shown in Figure 1. The N(amido)

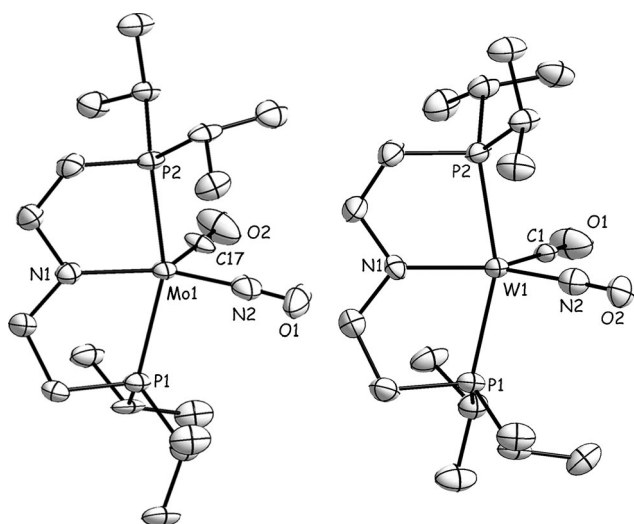


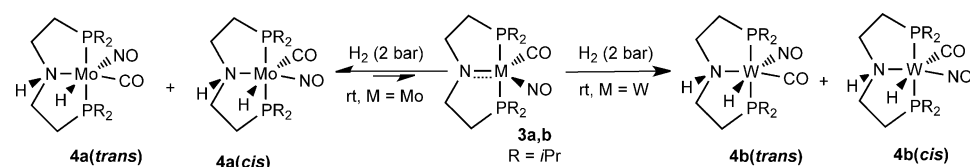
Figure 1. Molecular structures of [Mo(NO)(CO)(PNP)] (**3a**, left) and [W(NO)(CO)(PNP)] (**3b**, right); thermal ellipsoids are set at 50% probability. Selected bond lengths [Å] and angles [°] for compound **3a**: Mo1–N1 2.055(4), Mo1–N2 1.856(5), Mo1–C17 1.896(5), C17–O2 1.170(6); N1–Mo1–N2 140.34(18), P1–Mo1–P2 158.59(5), N2–Mo1–C17 91.2(2). Selected bond lengths [Å] and angles [°] for compound **3b**: W1–N1 2.061(5), W1–N2 1.882(5), W1–C1 1.869(6), C1–O1 1.182(6); N1–W1–N2 139.1(2), P1–W1–P2 158.81(6), N2–W1–C1 91.3(2).

atoms have shorter distances to the metal centers than the N(amine) atoms in compounds **1a,b** (see the Supporting Information), thus indicating $p_{\pi}(\text{N})-d_{\pi}(\text{M})$ double-bond character.

Low $\nu(\text{CO})$ stretching frequencies of compounds **3a,b** indicated that the CO groups were located in the trigonal plane of overall pseudo-trigonal-bipyramidal coordination geometries with significantly “deviated” equatorial $\text{C}_{\text{CO}}-\text{M}-\text{N}_{\text{NO}}$ angles close to 90° in the $16e^-$ *cis*-labilization intermediates.^[24]

Reactions of Compounds **3a** and **3b** with Hydrogen

Compound **3a** reacted slowly with H_2 (2 bar) at room temperature to form pseudo-octahedral complexes *cis*-[Mo(NO)(CO)H(PN^HP)] (**4a(cis)**) and *trans*-[Mo(NO)(CO)H(PN^HP)] (**4a(trans)**), which showed a hydride atom at the Mo center and a NH group on the PNP ligand. Heterolytic H_2 splitting across the $\text{M}=\text{N}$ bond had occurred (Scheme 2). $^{31}\text{P}\{^1\text{H}\}$ NMR analysis within the first 15 min of the reaction displayed one signal at $\delta=78.5$ ppm, owing to the formation of isomer **4a(trans)**, with H_2 approaching the $\text{Mo}=\text{N}$ bond from the CO-ligand side. After



Scheme 2. H_2 activation by amido complexes **3a** and **3b**.

30 min, an additional resonance was observed at $\delta=78.9$ ppm, thus indicating the build-up of isomeric product **4a(cis)** (8% with respect to **4a(trans)**, according to the ^{31}P NMR spectrum), with H_2 approaching from the NO side. The ^1H NMR spectra of the mixture of **4a(trans)** and **4a(cis)** revealed two triplets at $\delta=0.8$ ($^2J(\text{P,H})=26.3$ Hz) and -1.8 ppm ($^2J(\text{P,H})=26.3$ Hz), which were assigned to the hydride ligands of both complexes. These signals became singlets in the phosphorus-decoupled ^1H NMR spectra. Furthermore, the $^1\text{H}-^{31}\text{P}$ correlation spectra confirmed that the two hydride signals correlated with different $^{31}\text{P}\{^1\text{H}\}$ NMR signals, which again indicated the presence of two isomers. During the initial hour of the reaction, the intensities of the $^{31}\text{P}\{^1\text{H}\}$ NMR signals of compounds **4a(trans)** and **4a(cis)** changed further, which was explained on the basis of **4a(trans)**, as the kinetic isomer, forming faster and then slowly converting into a thermodynamic 1:1 mixture of both isomers (**4a(trans)** and **4a(cis)**). The equilibrium state could only be achieved for a 0.08 M solution of compound **3a** under 2 bar H_2 in $[\text{D}_8]\text{THF}$ after 30 h. DFT calculations also revealed that there was no significant energy difference between structures **4a(trans)** and **4a(cis)** ($\Delta E=0.01$ kcal mol^{-1} , see the Supporting Information). A plot of the change in the signal intensities in the ^{31}P NMR spectrum of **4a(trans)** and **4a(cis)** with time is shown in the Supporting Information, Figure S4. Notably, when the equilibrium mixture of compounds **4a(trans)**, **4a(cis)**, and **3a** was left under a H_2 atmosphere (2 bar), the constituents were present in a 7:7:6 equilibrium ratio, even after 5 days. However, compounds **4a(cis)** and **4a(trans)** were only stable in a H_2 atmosphere, which prevented their isolation. Thus, they were characterized in solution by ^1H and $^{31}\text{P}\{^1\text{H}\}$ NMR spectroscopy. The equilibration process of the **4a(trans)/4a(cis)** mixture was thought to proceed through the dissociation of H_2 from **4a(trans)** then re-addition from the NO side to form **4a(cis)**.

When compound **3b** was pressurized with H_2 (2 bar) and left for 1 h at room temperature, two signals were observed in the $^{31}\text{P}\{^1\text{H}\}$ NMR spectrum at $\delta=64.7$ and 65.4 ppm, which corresponded to **4b(trans)** and **4b(cis)**, respectively in a 4:1 ratio. Unlike in the Mo case, complete disappearance of the starting material was observed and no change in the intensities of the $^{31}\text{P}\{^1\text{H}\}$ NMR signals of **4b(trans)** and **4b(cis)** occurred, even after several weeks, thus suggesting the complete formation of the products and excluding an equilibrium for the H_2 addition. The ^1H NMR spectra exhibited two triplets at $\delta=2.85$ ($^2J(\text{P,H})=25.5$ Hz) and 2.75 ppm ($^2J(\text{P,H})=22.0$ Hz), which were attributed to the hydride ligands of **4b(trans)** and **4b(cis)**, respectively. In the IR spectra, one characteristic $\nu(\text{WH})$ band appeared at 1612 cm^{-1} for both isomers **4b(cis)** and **4b(trans)**, along with one sharp signal at 1556 cm^{-1} , which was assigned to the nitrosyl stretching vibrations, in accordance with similar

tungsten complexes reported earlier by ourselves.^[25] These complexes were stable under nitrogen atmosphere, but could not be separated. The ratio of isomers **4b(trans)** and **4b(cis)** was approximately the same as the initial ratio. We attempted to change the apparently kinetically determined ratio in the **4b(trans)/4b(cis)** mixture by heating compound **3b** to 140 °C and 60 bar H₂. After a reaction time of 20 min and immediate cooling of the mixture, the ³¹P NMR spectrum revealed a **4b(trans)/4b(cis)** ratio of 3:2 ($\Delta E = 0.4$ kcal mol⁻¹ from DFT calculations, see the Supporting Information).

Catalytic Hydrogenation of Imines

Next, we found that compounds **3a** and **3b** could be efficiently used for the catalytic hydrogenation of imines without the addition of a co-catalyst. The catalytic activity of compound **3a** was tested in initial room-temperature experiments to probe the hydrogenation of *N*-benzylideneaniline under 60 bar H₂ pressure in toluene with a loading of 2 mol% of catalyst **3a**. After a reaction time of 1 h, GCMS analysis of the reaction mixture revealed the formation of phenylbenzylamine as the hydrogenated product, but it was obtained in a low 30% yield with a low maximum TOF of 15 h⁻¹. The reaction went to completion within 3.5 h (Table 1, entry 1). Under the same conditions but with catalyst **3b**, only 25% phenylbenzylamine was obtained after 12 h, with a TOF of 1 h⁻¹ (Table 1, entry 2). To improve the performance of the hydrogenation of imines catalyzed by

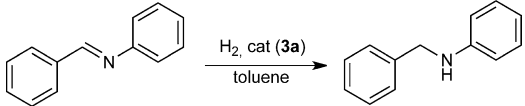
compounds **3a** or **3b** at room temperature, higher catalyst loadings were envisaged and also longer reaction times to achieve full conversions. Indeed, when the temperature was increased to 140 °C, the catalytic activities of compounds **3a** and **3b** were boosted.

Optimization experiments showed that the hydrogenation of *N*-benzylideneaniline could be greatly improved by applying higher temperatures (80–140 °C) and H₂ pressures (20–60 bar). These catalytic hydrogenation reactions seemed to work best in aprotic solvents, because no hydrogenation was observed in isopropanol, MeOH, or EtOH. Eventually, a temperature of 140 °C and 60 bar H₂ pressure were found to be the optimum conditions, thereby achieving a maximum TOF of 1600 h⁻¹ for the hydrogenation of *N*-benzylideneaniline in toluene (Table 1, entry 6). Aware of the previous work in our group on rhenium complexes, in which dramatic improvements in the catalytic hydrogenation of olefins were observed by using B(C₆F₅)₃ or R₃SiH/B(C₆F₅)₃ as co-catalysts,^[19a,26] we also attempted to accelerate the imine-hydrogenation reaction in the same manner. However, the addition of co-catalysts led to a decrease in the catalytic activity. A loading of 0.17 mol% of compound **3a** in the presence of B(C₆F₅)₃ or a Et₃SiH/B(C₆F₅)₃ mixture as a co-catalyst led to TOFs of 528 and 576 h⁻¹, respectively (Table 1, entries 7 and 8) in the hydrogenation of *N*-benzylideneaniline under 60 bar H₂ at 140 °C.

Next, several other imines were also tested by using catalysts **3a** and **3b** under the same conditions as above without the addition of any co-catalyst, although the catalyst loadings were varied to achieve optimum performance (Table 2). Complex **3a** showed the highest catalytic activity for the hydrogenation of *N*-(4-methoxybenzylidene)aniline, with a maximum TOF of 2912 h⁻¹ (Table 2, entry 19), which is the highest reported TOF for a Mo-based hydrogenation catalyst to date. Various *para*-substituted imines (*p*-ClC₆H₄CH=N-*p*-C₆H₄Cl, PhCH=N-(α -Np), *p*-MeOC₆H₄CH=NPh, PhCH=N-*p*-C₆H₄OMe, *p*-ClC₆H₄CH=NPh, PhCH=N-*p*-C₆H₄Cl, *p*-MeOC₆H₄CH=N-*p*-C₆H₄OMe, *p*-MeOC₆H₄CH=N-*p*-C₆H₄Cl, *p*-ClC₆H₄CH=N-*p*-C₆H₄OMe, *p*-FC₆H₄CH=NPh, and PhCH=N-*p*-C₆H₄F) were fully converted into their corresponding amines in less than 1 h at 140 °C under 60 bar H₂. *p*-NO₂C₆H₄CH=NPh was not reduced (Table 2, entry 27).

The catalytic performance of compound **3a** for the hydrogenation of carbonyl functionalities was also tested, but these transformations were much less effective. Acetophenone was hydrogenated into 1-phenylethanol in 32% yield after 3.5 h with 1 mol% loading of catalyst **3a** at 140 °C under 60 bar H₂ in toluene. However, the maximum initial TOF was only 14 h⁻¹ (Table 1, entry 10). No hydrogenation was observed when benzaldehyde was used as a substrate with catalyst **3a** at 140 °C and 60 bar H₂.

Table 1. Optimization of the imine hydrogenation conditions using catalyst **3a**.



Entry	S/C	T [°C]	P [bar]	TOF ^[a] [h ⁻¹]	Conversion ^[b] [%]
1 ^[c]	50	RT	60	15	100
2 ^[d]	50	RT	60	1	25
3	100	80	60	208	52
4	200	100	60	540	68
5	600	140	20	1272	53
6	600	140	60	1600	68
7 ^[e]	600	140	60	528	22
8 ^[f]	600	140	60	576	24
9 ^[g]	400	140	60	1120	70
10 ^[h]	100	140	60	14	32
11 ^[i]	100	140	60	–	0

[a] TOFs were calculated from GCMS after an initial 15 min. [b] Conversions were determined by GCMS after 15 min, based on the consumption of the substrate. [c] The TOF was determined after 1 h and the conversion was determined after 3.5 h by GCMS. [d] Compound **3b** was used as the catalyst; conversion was determined after 12 h and the TOF was calculated from the conversion after 12 h. [e] B(C₆F₅)₃ was used as a co-catalyst. [f] Et₃SiH/B(C₆F₅)₃ was used as the co-catalyst. [g] THF was used as the solvent. [h] Acetophenone was used as the substrate and the TOF was calculated after 1 h. [i] Benzaldehyde was used as the substrate. S/C = substrate/catalyst molar ratio.

Table 2. Hydrogenation of various imines by using catalysts **3a**, **3b**, and mixture of compounds **4b(cis)** and **4b(trans)** under the optimized conditions.

		$\text{Ar}-\text{CH}=\text{N}-\text{Ar} \xrightarrow[\text{cat, toluene}]{60 \text{ bar } \text{H}_2, 140 \text{ }^\circ\text{C}} \text{Ar}-\text{CH}_2-\text{NH}-\text{Ar}$				
Entry	Substrate	Cat.	S/ C	TOF ^[a] [h ⁻¹]	<i>t</i> [h]	Conversion ^[b] [%]
12	PhCH=NPh	3a	600	1600	< 0.5	> 97
13	PhCH=NPh	3b	200	424	< 1	> 99
14 ^[c]	PhCH=NPh	4b	200	356	1	99
15	<i>p</i> -ClC ₆ H ₄ CH=N- <i>p</i> -C ₆ H ₄ Cl	3a	400	480	< 1	> 99
16	<i>p</i> -ClC ₆ H ₄ CH=N- <i>p</i> -C ₆ H ₄ Cl	3b	400	464	< 1	> 99
17	PhCH=N-(α -Np)	3a	200	792	0.25	> 99
18	PhCH=N-(α -Np)	3b	200	112	1	> 98
19	<i>p</i> -MeOC ₆ H ₄ CH=NPh	3a	800	2912	0.5	> 99
20	<i>p</i> -MeOC ₆ H ₄ CH=NPh	3b	400	1120	< 1	> 99
21 ^[d]	PhCH=N- <i>p</i> -C ₆ H ₄ OMe	3a	600	1440	< 1	> 99
22	<i>p</i> -ClC ₆ H ₄ CH=NPh	3a	200	496	< 1	> 98
23	PhCH=N- <i>p</i> -C ₆ H ₄ Cl	3a	800	1979	< 1	> 97
24	<i>p</i> -MeOC ₆ H ₄ CH=N- <i>p</i> -C ₆ H ₄ OMe	3a	200	546	< 1	77
25 ^[d]	<i>p</i> -ClC ₆ H ₄ CH=N- <i>p</i> -C ₆ H ₄ OMe	3a	100	332	< 1	> 99
26	<i>p</i> -MeOC ₆ H ₄ CH=N- <i>p</i> -C ₆ H ₄ Cl	3a	200	744	0.25	> 93
27	<i>p</i> -NO ₂ C ₆ H ₄ CH=NPh	3a	50	–	14	0
28	<i>p</i> -FC ₆ H ₄ CH=NPh	3a	200	712	< 1	99
29	PhCH=N- <i>p</i> -C ₆ H ₄ F	3a	800	1920	< 1	> 99
30	PhCH=N <i>t</i> Bu	3a	50	–	1	0

[a] TOFs were calculated by GCMS after an initial 15 min. [b] Conversions were determined by GCMS, based on the consumption of the substrates. [c] **4b** = mixture of **4b(cis)** and **4b(trans)**. [d] TOFs and conversions were determined by integration of the ¹H NMR spectra. Np = naphthyl.

Mechanistic Studies of Imine Hydrogenation

Hammett Correlations for the Imine-Hydrogenation Reactions

To conclude our mechanistic investigation and to understand the electronics of the imine-hydrogenation process, we explored the influence of various *para* substituents on the aromatic imines by using Hammett^[27] correlations (Figure 2) with catalyst **3a** and a series of *p*-H, *p*-OMe-, *p*-F-, and *p*-Cl-substituted *N*-benzylideneanilines that were substituted on both the benzylidene and aniline sides. The initial rates (in s⁻¹) were obtained from the TOF (h⁻¹) values (TOF = reaction rate normalized by the catalyst concentration). The Hammett correlations were established by plotting the ln(hydrogenation rate) versus the substituent constant (σ), which gave a straight line with a negative slope of -3.69 for *para* substitution on the benzylidene side.

Para substitution on the aniline side also gave a straight line, but with a positive slope of 0.68. The Hammett parameter (ρ) indicates the susceptibility of a transformation towards the electronic influence of the substituents. A negative ρ value greater than 1 indicates the build-up of positive charge at the reaction center in the transition state and that the rate of the reaction is enhanced by the presence of elec-

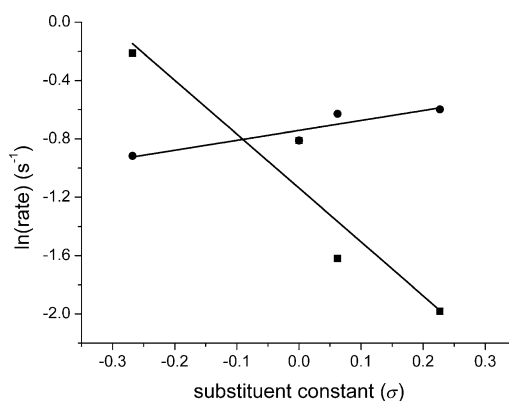


Figure 2. Hammett plot for the hydrogenation of various *para*-substituted imines catalyzed by compound **3a**, as extracted from the initial TOF values. ■: $\rho = -3.69$, hydrogenation reactions with *para* substitution on the benzylidene side; ●: $\rho = 0.68$, hydrogenation reactions with *para* substitution on the aniline side. Left to right: *p*-MeO, *p*-H, *p*-F, and *p*-Cl groups.

tron-donating groups, whereas a positive ρ value indicates the build-up of negative charge at the reaction center and that the rate of the reaction is enhanced by electron-withdrawing groups. As expected, for the hydrogenation of benzylideneaniline, an electron-donating group on the benzylidene side and an electron-withdrawing group on the aniline side increased the overall rate (Table 2, entries 19, 21–23, 25, 26, 28, and 29), thereby affording a strongly polarized C=N bond in the transition



Kinetic Studies

The dependence of the hydrogenation rate on the concentrations of amido complex **3a** and *N*-benzylideneaniline, as well as on H₂ pressure, were investigated in toluene at 140 °C; the conversion of the imine was monitored by ¹H NMR spectroscopy and GCMS analysis. Initially, five kinetic experiments were carried out by varying the concentration of *N*-benzylideneaniline whilst keeping the concentration of the catalyst and H₂ pressure fixed at 2 bar (see the Supporting Information, Table S2, runs 1–5). Furthermore, the initial rates were determined by varying the concentration of the catalyst whilst keeping the concentration of *N*-benzylideneaniline fixed under 2 bar H₂ (see the Supporting Information, Table S2, runs 2, 6–9). The initial rate data (see the Supporting Information, Table S2) revealed that the rate of the reaction was independent of the substrate concentration, but varied with the catalyst concentration: zeroth order in the substrate and first order in catalyst **3a**.

A typical kinetic plot of the concentration of *N*-benzylideneaniline over time and the dependence of the initial rate on the catalyst concentration (at a fixed substrate concentration) are shown in Figure 3.

The dependence of the reaction on H₂ pressure was also investigated by determining the initial rates at 20, 40, and 60 bar H₂ pressures, whilst keeping all other concentrations

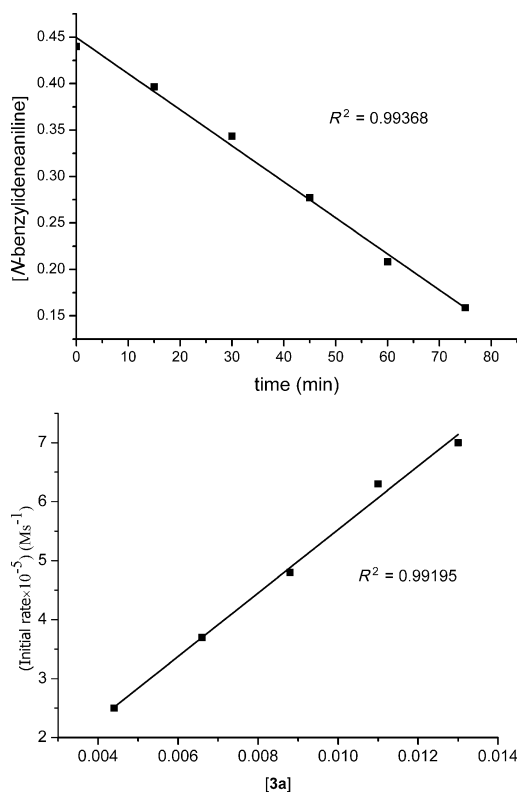


Figure 3. Top: Kinetic plot of the concentration of *N*-benzylideneaniline over time; initial [*N*-benzylideneaniline] = 0.44 M, [**3a**] = 0.0088 M, 2 bar H_2 , 140 °C. Bottom: Plot of the initial rates at various concentrations of catalyst **3a**; [*N*-benzylideneaniline] = 0.44 M, 2 bar H_2 , 140 °C.

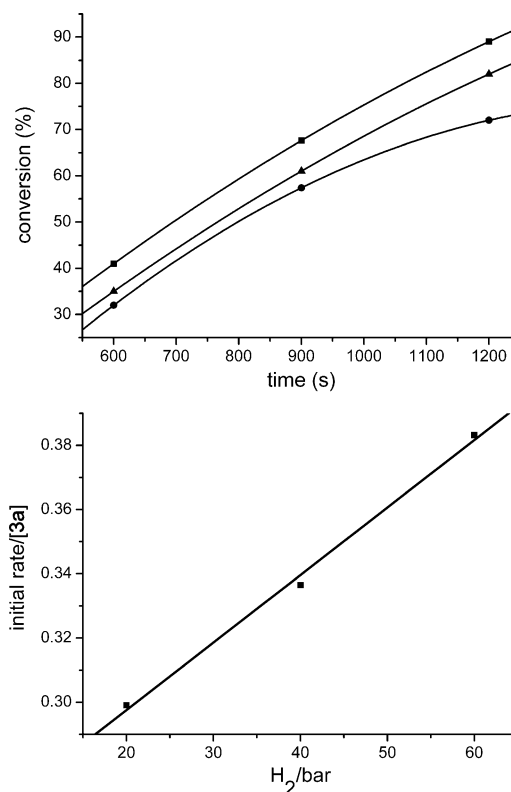


Figure 4. Top: Kinetic conversion chart of *N*-benzylideneaniline catalyzed by compound **3a** at 140 °C. ■: 60 bar H_2 ; ▲: 40 bar H_2 ; ●: 20 bar H_2 . Bottom: Plot of the initial rate/[**3a**] versus H_2 pressure.

constant (see the Supporting Information, Table S3). A plot of the initial rate/[**3a**] versus hydrogen pressure is shown in Figure 4, right. This result indicated that the reaction rate was also dependent on hydrogen pressure.

Stoichiometric Model Experiments

To further investigate the mechanism of the catalytic reaction, stoichiometric experiments were carried out. For example, equal amounts of catalyst **3a** and *N*-benzylideneaniline were left to stand at room temperature for 1 h, but no change was observed in the ^1H and ^{31}P NMR spectra. Even heating of the stoichiometric mixtures to 140 °C for a minimum of 3 h did not induce any changes in the ^{31}P and ^1H NMR spectra, which excluded the possibility of direct binding of the substrate to the catalytic metal center and also revealed that the binding was not a step in the catalytic reaction.

Additional mechanistic studies were expected to clarify the H-transfer sequence from the NH–MoH moiety, that is, whether it occurred stepwise or simultaneously. First, though, we had to examine whether the H-transfers onto the imine were rate limiting. For this purpose, we chose compounds **4b(cis)** and **4b(trans)** as a model system because hydride species **4a(cis)** and **4a(trans)** were only stable under a H_2 atmosphere, which would complicate the measurements. Initially, a 0.018 M solution of compound **3b** in

$[\text{D}_8]\text{THF}$ was filled with 2 bar H_2 and left to stand for several hours at room temperature. After a reaction time of 90 h, complete conversion of compound **3b** into hydride species **4b(cis)** and **4b(trans)** was observed. Then, the hydrogen pressure was released and 10 equivalents of *N*-benzylideneaniline were added with stirring. After 10 min, the ^{31}P NMR spectra of the reaction mixture revealed the complete disappearance of the signals of **4b(cis)** and **4b(trans)**. The presence of the signal of compound **3b** at $\delta = 82$ ppm indicated complete H-transfer from the hydride species to the *N*-benzylideneaniline and regeneration of the amide species. In addition, the ^1H NMR spectra of the reaction mixture confirmed the presence of phenylbenzylamine, along with the remaining *N*-benzylideneaniline.

Again, when the hydrogenation of *N*-benzylideneaniline (40 equiv with respect to the catalyst) was carried out with catalysts **3a** and **3b** (5 mg in $[\text{D}_8]\text{toluene}$) under 2 bar H_2 at 140 °C for 15 min, 28% and 15% conversions of *N*-benzylideneaniline into phenylbenzylamine were observed, respectively, with the catalysts as the only other detectable species. Catalysts **3a** or **3b** and *N*-benzylideneaniline and phenylbenzylamine were identified during the catalytic reactions at 140 °C and 60 bar H_2 at an incomplete stage of conversion. Therefore, catalysts **3a** and **3b** are presumed to be the active species that accumulate before the rate-determining step. In contrast, hydride complexes of type **4** were considered to be relatively short-lived intermediates, because the

transfer of the hydrogen atoms onto the imines was apparently fast. If the hydride transfer would be rate limiting, one would expect that they would accumulate during the catalytic reaction,^[28,17a] which we did not observe.

To compare the reaction kinetics of catalyst **3b** and hydride complexes **4b(cis)**/**4b(trans)**, catalytic experiments were carried out in toluene at 140 °C and 60 bar H₂. An initial TOF of 356 h⁻¹ was obtained for the hydrogenation of *N*-benzylideneaniline with the mixture of **4b(cis)** and **4b(trans)**, whereas the TOF was 424 h⁻¹ with catalyst **3b** (Table 2, entries 13 and 14). Thus, there was a slight difference between the catalytic activities, but we did not think that this difference was significant, because it might have originated from the fact that the mixture of hydride complexes **4b(cis)** and **4b(trans)** in toluene was less soluble than complex **3b**.

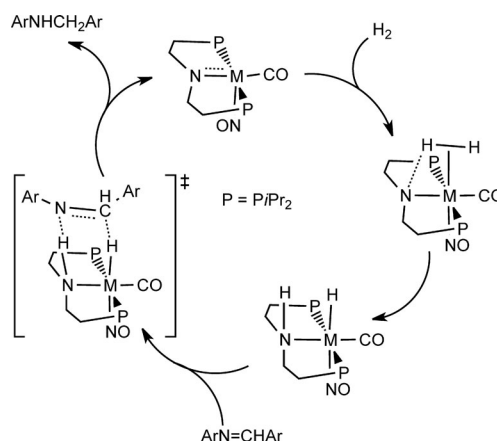
Deuterium Kinetic Isotope Effect Experiments

To gain further insight into the deuterium isotope kinetics, we performed the hydrogenation of *N*-benzylideneaniline catalyzed by compound **3a** at 140 °C with 20 bar of H₂ or D₂. A loading of 0.5 mol % of catalyst **3a** to a solution of *N*-benzylideneaniline in toluene led to a TOF of 756 h⁻¹ under 20 bar D₂, which corresponded to a DKIE of $k_H/k_D=1.28$, that is, a very small kinetic isotope effect. This result might imply that H–H bond splitting is not directly involved in the rate-limiting step, because the KIEs of reactions with rate-determining H₂ splitting generally give relatively high positive values.

In separate experiments, we also reacted 2 bar of H₂ or D₂ at room temperature with a 0.03 M solution of compound **3b** in THF (6.5 mg of **3b** in 0.4 mL THF). After 72 h, 89 % formation of hydride complexes **4b(cis)** and **4b(trans)** was observed for the H₂ reaction and, in a related experiment with D₂, 73 % formation of deuterated type-4 compounds was observed, as indicated by the ³¹P NMR spectra, which corresponded to a k_H/k_D value of 1.22. This low DKIE value of the H₂ and D₂ reactions to form the type-4 hydride complexes supported the conclusion that any type of H₂ splitting did not participate in the rate-determining step.

Therefore, it was quite plausible to assume that the addition steps of H₂ to the amido complexes of type **3** were rate determining,^[4c,29] which consisted of initial H₂ uptake to the molybdenum center. Then, heterolytic splitting of the H₂ ligand would occur through proton abstraction by the basic amido nitrogen atom. The H₂-addition step was assumed to be accompanied by extensive structural rearrangement, which would transform the trigonal-bipyramidal geometry of the amido complex into an octahedral geometry. The concomitant rearrangement energy was naturally independent of the H₂-splitting step, but apparently higher in energy than the heterolysis of H₂.

Based on the kinetic studies, mechanistic experiments, and Hammett correlations, a secondary-coordination-sphere mechanism analogous to Noyori's bifunctional catalysis is proposed for the H-transfers onto the imine moieties, as shown in Scheme 3.



Scheme 3. Proposed mechanism for the imine-hydrogenation reaction.

Filtration Experiments as Homogeneity Tests of the Imine-Hydrogenation Reactions

Filtration experiments^[30] were carried out to exclude any heterogeneous side-reactions during the hydrogenation catalysis. For this purpose, 1 mol % of catalyst **3b** was loaded at 140 °C under 60 bar H₂ for the hydrogenation of *N*-benzylideneaniline. After 7 min, the vessel was immediately cooled to room temperature and moved into a glove box. The reaction mixture was still a red color and there were no visible precipitates. GCMS analysis of the reaction mixture showed 50 % conversion of the imine into the corresponding amine. The ³¹P and ¹H NMR spectra only revealed the presence of compound **3b**. After filtration of the solution, the experiment was repeated once more, but showed no black precipitates or dark solutions, thus making the formation of metal particles less plausible.

Conclusions

We have developed highly efficient non-platinum-metal catalysts for imine-hydrogenation reactions by using molybdenum- and tungsten-amido complexes. Reactive amido complexes of the type [M(NO)(CO)(PNP)] (M=Mo, **3a**; W, **3b**) were prepared by the dehydrohalogenation of compounds **1a,b** by using Na[N(SiMe₃)₂]. These amido complexes cleaved dihydrogen in a heterolytic fashion across the polar M=N double bond to generate hydride-amine complexes with a formal 1,2-addition that was related to frustrated Lewis pairs.^[31] Amido complexes **3a,b** could be used as excellent imine-hydrogenation catalysts. Detailed kinetic studies, mechanistic investigations, and Hammett studies supported the H-transfer onto the imine through a secondary-coordination-sphere mechanism, similar to Noyori-type metal–ligand bifunctional catalysis, whilst the addition of hydrogen did not proceed through a secondary-coordination-sphere-type mechanism; rather, the addition to the metal center was the rate-determining step, with considerable rearrangement of the coordination sphere.

Experimental Section

General Procedures

All experiments were carried out under a N₂ atmosphere by using either glove-box or Schlenk techniques. Reagent-grade solvents benzene, THF, pentane, toluene, and Et₂O were dried with sodium benzophenone and distilled prior to use under a N₂ atmosphere. Anhydrous toluene (99.8%, active dry) for the catalytic experiments was purchased from Alfa Aesar. CH₂Cl₂ was dried over calcium hydride and distilled. Deuterated solvents were dried with sodium benzophenone ketyl ([D₈]THF, [D₈]toluene, and C₆D₆) and calcium hydride (CD₂Cl₂) and distilled by a freeze-pump-thaw cycle prior to use. The [M(NO)(CO)₄(ClAlCl₃)] (M = Mo, W) complexes and HN(CH₂CH₂iPr)₂ were prepared according to literature procedures.^[32] KOtBu and Na[N(SiMe₃)₂] were purchased from commercially available sources and used without further purification. NMR spectra were measured on Varian Mercury 200 (200.1 MHz for ¹H and 81.0 MHz for ³¹P), Varian Gemini-300 (300.1 MHz for ¹H and 75.4 MHz for ¹³C), Bruker-DRX 500 (500.2 MHz for ¹H, 202.5 MHz for ³¹P, and 125.8 MHz for ¹³C), and Bruker-DRX 400 spectrometers (400.1 MHz for ¹H, 162.0 MHz for ³¹P, and 100.6 MHz for ¹³C). All ¹H and ¹³C[¹H] chemical shifts are expressed in ppm relative to tetramethylsilane (TMS); ³¹P[¹H] chemical shifts are expressed relative to 85% H₃PO₄ as an external standard. Signal multiplicities are expressed as followed: s singlet, d doublet, t triplet, q quartet, m multiplet. IR spectra were obtained by using either the ATR or KBr methods on a Bio-rad FTS-45 instrument. Elemental analysis was carried out at the Anorganisch-Chemisches Institut of the University of Zurich. GCMS spectra were recorded on a Varian Saturn 2000 spectrometer that was equipped with a Varian 450-GC chromatograph (Phenomenex ZB-5ms (30 m), Gradient 70–270°).

General Procedure for the Preparation of [M(NO)(CO)Cl(PN^HP)] (M = Mo, **1a**; W, **1b**)

To a solution of [M(NO)(CO)₄(ClAlCl₃)] (1.23 mmol) in THF (15 mL) was added a solution of HN(CH₂CH₂iPr)₂ (1.23 mmol) in THF (5 mL) and the resulting mixture was heated at 90°C for 3 h. After the completion of the reaction, the resulting red solution was filtered off and evaporated to dryness. The solid residue was washed twice with pentane then dissolved in a minimum amount of THF and pentane was added. The solid precipitate was separated and dried in vacuo.

1a: Yield: 450 mg (74%); ¹H NMR (400 MHz, [D₈]THF): δ = 3.7 (br s; NH, minor isomer), 3.47–3.36 (m; NCH₂), 3.2 (br s; NH, major isomer), 2.68–2.53 (m; NCH₂), 2.41–2.37 (m; CH), 1.78–1.66 (m; PCH₂), 1.36–1.23 ppm (m; CH₃); ¹³C[¹H] NMR (100.6 MHz, [D₈]THF): δ = 246.89 (t, ²J(C,P) = 7.2 Hz; CO), 50.95 (t, ¹J(C,P) = 4.8 Hz; NCH₂), 25.69 (t, ¹J(C,P) = 7.2 Hz; CH), 21.56 (t, ¹J(C,P) = 8.5 Hz; PCH₂), 18.23 (t, ¹J(C,P) = 3.6 Hz; CH₃); ³¹P[¹H] NMR (161.9 MHz, [D₈]THF): δ = 60.17 (s; major isomer), 59.09 ppm (s; minor isomer); IR (KBr): $\tilde{\nu}$ = 1573 (NO), 1912 cm⁻¹ (CO); elemental analysis calcd (%) for C₁₇H₃₇ClMoN₂O₂P₂: C 41.26, H 7.54, N 5.66; found: C 41.09, H 7.43, N 5.37.

1b: Yield: 560 mg (78%); ¹H NMR (500 MHz, [D₈]THF): δ = 4.3 (s; NH, major isomer), 3.7 (s; NH, minor isomer), 3.46–3.50 (m; NCH₂), 2.73–2.64 (m; NCH₂), 2.57–2.46 (m; CH), 1.79–1.78 (m; PCH₂), 1.24–1.38 ppm (m; CH₃); ¹³C[¹H] NMR (100.61 MHz): δ = 246.46 (t, ²J(C,P) = 3.6 Hz; CO), 52.59 (t, ¹J(C,P) = 4.8 Hz; NCH₂), 27.03 (t, ¹J(C,P) = 8.3 Hz; CH), 23.53 (s), 21.77 (t, ¹J(C,P) = 9.5 Hz; CH₂), 19.80 (t, ¹J(C,P) = 9.5 Hz; CH₂), 18.25 (t, ²J(C,P) = 3.6 Hz; CH₃), 16.71 (s; CH₃), 15.38 (s; CH₃); ³¹P[¹H] NMR (161.9 MHz, [D₈]THF): δ = 52.03 (s, ¹J(P,W) (d, satellite) = 305.9 Hz, major isomer), 51.0 ppm (s, ¹J(P,W) (d, satellite) = 302.9 Hz, minor isomer); IR (KBr): $\tilde{\nu}$ = 1556 (NO), 1894 cm⁻¹ (CO); elemental analysis calcd (%) for C₁₇H₃₇ClN₂O₂P₂W: C 35.04, H 6.40, N 4.81; found: C 34.98, H 6.21, N 5.13.

Synthesis of [Mo(NO)(CO)(PN^HP)(OtBu)] (**2a**)

Compound **1a** (0.1 g, 0.20 mmol) and KOtBu (0.035 g, 0.30 mmol) were mixed in THF (10 mL) in a Schlenk flask and the mixture was stirred for 2 h at RT. After completion of the reaction, the solution was filtered off and the solvent was removed in vacuo. The crude product was dissolved

in Et₂O and filtered. Then, the solution was concentrated and stored in the fridge at –30°C. Yellow single crystals suitable for X-ray diffraction were obtained after several days. Yield: 69 mg (65%); ¹H NMR (400 MHz, [D₈]THF): δ = 4.9 (br s, 1H; NH), 3.40–3.29 (m; NCH₂), 2.69–2.64 (m, 2H; NCH₂), 2.45–2.33 (m, 4H; CH), 1.62–1.53 (m, 4H; PCH₂), 1.37–1.19 (m; CH₃), 0.99 ppm (s; CH₃); ¹³C[¹H] NMR (100.6 MHz): δ = 246.91 (t, ²J(C,P) = 7.2 Hz; CO), 26.03 (t, ¹J(C,P) = 5.9 Hz; CH), 23.57 (t, ¹J(C,P) = 7.2 Hz; CH₂), 20.94 (t, ¹J(C,P) = 7.2 Hz; CH₂), 18.76 (t, ¹J(C,P) = 4.8 Hz; CH₃), 17.72 (t, ¹J(C,P) = 2.4 Hz; CH₃), 17.01 ppm (s; CH₃); ³¹P[¹H] NMR (161.9 MHz, [D₈]THF): δ = 50.98 ppm (s); IR (KBr): $\tilde{\nu}$ = 1558 (NO), 1883 cm⁻¹ (CO); elemental analysis calcd (%) for C₂₁H₄₇MoN₂O₃P₂: C 47.28, H 8.88, N 5.25; found: C 46.90, H 8.60, N 5.01.

General Procedure for the Preparation of [M(NO)(CO)(PN^HP)] (M = Mo, **3a**; W, **3b**)

To a solution of [M(NO)(CO)(PN^HP)Cl] (0.81 mmol) in THF was added Na[N(SiMe₃)₂] (1.22 mmol, 1.5 equiv, 1 M in THF) and the resulting mixture was stirred for 30 min. After the completion of the reaction (by ³¹P[¹H] NMR spectroscopy), the product was filtered and dried in vacuo. Then, the desired product was extracted with pentane. Finally, it was concentrated and stored in the fridge at –30°C. Red crystals were obtained after several days.

3a: Yield: 210 mg (57%); ¹H NMR (500 MHz, [D₈]THF): δ = 3.50–3.42 (m, 2H; NCH₂), 3.36–3.28 (m, 2H; NCH₂), 2.36–2.23 (m, 4H; CH), 2.11–2.04 (m, 2H; PCH₂), 1.98–1.92 (m, 2H; PCH₂), 1.069–1.387 ppm (m, 24H; CH₃); ¹³C[¹H] NMR (125.8 MHz, [D₈]THF): δ = 60.5 (t, ¹J(C,P) = 8.3 Hz; NCH₂), 23.87 (m; CH), 21.29 (t, ¹J(C,P) = 8.3 Hz; CH₂), 16.2 (m; CH₃), 15.3 ppm (m; CH₃); ³¹P[¹H] NMR (161.9 MHz, [D₈]THF): δ = 82.01 ppm (s); IR (KBr): $\tilde{\nu}$ = 1565 (NO), 1893 cm⁻¹ (CO); elemental analysis calcd (%) for C₁₇H₃₆MoN₂O₂P₂: C 44.54, H 7.92, N 6.11; found: C 44.74, H 8.01, N 6.23. Assignments in the ¹H NMR spectrum were confirmed by C-H correlations, long-range C-H correlations, and ¹³C DEPT experiments.

3b: Yield: 238 mg (54%); ¹H NMR (400 MHz, [D₈]THF): δ = 3.52–3.44 (m, 2H; NCH₂), 3.36–3.27 (m, 2H; NCH₂), 2.46–2.32 (m, 4H; CH), 2.11–2.05 (m, 2H; PCH₂), 2.02–1.93 (m, 2H; PCH₂), 1.29–1.13 ppm (m, 24H; CH₃); ¹³C[¹H] NMR (100.61 MHz, [D₈]THF): δ = 253.6 (s; CO), 63.36 (t, ¹J(C,P) = 8.3 Hz; NCH₂), 25.06 (t, ¹J(C,P) = 11.9 Hz; CH), 24.43 (t, ¹J(C,P) = 10.7 Hz; CH), 21.73 (m; CH₂), 16.21 (s; CH₃), 15.36 ppm (s; CH₃); ³¹P[¹H] NMR (162 MHz, [D₈]THF): 81.09 ppm (s, ¹J(P,W) (d, satellite) = 320.1 Hz); IR (KBr): $\tilde{\nu}$ = 1541 (NO), 1871 cm⁻¹ (CO); elemental analysis calcd (%) for C₁₇H₃₆N₂O₂P₂W: C 37.38, H 6.64, N 5.13; found: C 37.72, H 6.74, N 5.01.

Reaction of Compound **3a** with Hydrogen to form Compounds **4a(trans)** and **4a(cis)**

A solution of compound **3a** (18 mg, 0.039 mmol) in [D₈]THF (0.5 mL) in a J. Young NMR tube was frozen with liquid nitrogen. Then, the nitrogen atmosphere was removed by a freeze-pump-thaw cycle and the tube was filled with 2 bar H₂ and sealed. The tube was shaken vigorously and left for a few hours. The slow formation of compounds **4a(trans)** and **4a(cis)** was monitored by ³¹P[¹H] NMR spectroscopy. After 30 h, an equilibrium mixture of compounds **4a(cis)**, **4a(trans)**, and **3a** (1:1:1 ratio) was observed. The formation of compounds **4a(cis)** and **4a(trans)** was confirmed by ¹H and ³¹P NMR spectroscopy in solution, as well as by ³¹P-¹H correlation spectroscopy.

Selected ¹H NMR (500 MHz, [D₈]THF): δ = 0.8 (t, ²J_{PH} = 26.3 Hz; Mo-H, **4a(trans)**), –1.8 ppm (t, ²J_{PH} = 26.2 Hz; Mo-H, **4a(cis)**); ³¹P[¹H] NMR (202 MHz, [D₈]THF): δ = 78.5 (s; **4a(trans)**), 78.9 ppm (s, **4a(cis)**). Several of the signals in the ¹H NMR spectrum were in their expected regions, owing to presence of equilibrium mixtures of compounds **3a**, **4a(trans)**, and **4a(cis)**.

Synthesis of [W(NO)(CO)H(PN^HP)] (Mixture of Isomers **4b(cis)** and **4b(trans)**)

A solution of compound **3b** (30 mg, 0.056 mmol) in [D₈]THF (0.5 mL) in a J. Young NMR tube was frozen with liquid nitrogen. Then, the nitrogen atmosphere was removed by a freeze-pump-thaw cycle and the tube was

allowed to warm to RT. The tube was filled with 2 bar H₂ and sealed. The tube was shaken vigorously and left for a few hours. The formation of compounds **4b(cis)** and **4b(trans)** was supported by ¹H and ³¹P{¹H} NMR spectroscopy, as well as by ³¹P-¹H correlation spectroscopy. ¹H NMR (400 MHz, 298 K, [D₈]THF): δ = 3.5 (br s, 1H; NH, **4b(cis)**), 3.3 (br s, 1H; NH, **4b(trans)**), 3.02 (m; NCH₂), 2.85 (t, ²J(P,H) = 25.5 Hz; W-H, **4b(trans)**), 2.75 (t, ²J(P,H) = 22 Hz; W-H, **4b(cis)**), 2.44–1.99 (m; CH, CH₂), 1.29–1.23 ppm (m; CH₃); ¹³C{¹H} NMR (100.62, [D₈]THF): δ = 247.2 (s; CO), 53.89 (t, ^νJ(C,P) = 4.78 Hz; NCH₂), 31.10 (t, ^νJ(C,P) = 11.2 Hz; CH), 31.79 (t, ^νJ(C,P) = 13.1 Hz; CH), 28.52 (CH₂P), 20.64 (s; CH₃), 19.43 (s; CH₃), 18.56 (s; CH₃), 17.74 (s; CH₃); ³¹P{¹H} NMR (161.97 MHz, [D₈]THF): δ = 64.7 (s, ¹J(P,W) = 306.7 Hz; **4b(trans)**) 65.4 ppm (s; **4b(cis)**); IR (KBr): $\tilde{\nu}$ = 1556 (NO), 1618 (WH), 1864 (CO), 3422 cm⁻¹ (NH); elemental analysis calcd (%) for C₁₇H₃₈N₂O₂P₂W: C 37.24, H 6.99, N 5.11; found: C 36.89, H 7.03, N 5.19.

General Procedure for the Catalytic Imine-Hydrogenation Experiments

A stock solution of freshly prepared catalyst (10 mg in 2.5 mL toluene) was prepared. An aliquot (0.5 mL) of that stock solution was added to a solution of imines (according to substrate catalyst ratio) in 1.5 mL toluene in a steel autoclave. The autoclave was charged with required hydrogen pressure and kept in a preheated (140 °C) oil bath. After appropriate reaction times, the autoclave was immediately taken out and cooled to room temperature and the pressure was released. The reaction mixture was taken out of the autoclave and filtered through silica gel. Without further purifications, GC/MS analysis was measured to determine the conversion of the hydrogenation product and to identify the products.

GCMS Data for Various Imines and Amines that were Formed during Hydrogenation Reactions Catalyzed by Compounds **3a** and **3b**

PhCH=NPh: *t_r* = 9.062 min, *m/z* = 181; PhCH₂NHPh: *t_r* = 9.323 min, *m/z* = 183; PhCH=N(α-naphthyl): *t_r* = 13.260 min, *m/z* = 231; PhCH₂NH(α-naphthyl): *t_r* = 13.673 min, *m/z* = 233; *p*-ClC₆H₄CH=NPh: *t_r* = 10.284 min, *m/z* = 215; *p*-ClC₆H₄CH₂NHPh: *t_r* = 10.687 min, *m/z* = 217; PhCH=N-*p*-C₆H₄Cl: *t_r* = 10.362 min, *m/z* = 215; PhCH₂NH-*p*-C₆H₄Cl: *t_r* = 10.829 min, *m/z* = 217; *p*-ClC₆H₄CH=N-*p*-C₆H₄Cl: *t_r* = 11.815 min, *m/z* = 248; *p*-ClC₆H₄CH₂NH-*p*-C₆H₄Cl: *t_r* = 12.648 min, *m/z* = 251; *p*-MeOC₆H₄CH=NPh: *t_r* = 10.934 min, *m/z* = 211; *p*-MeOC₆H₄CH₂NHPh: *t_r* = 11.012 min, *m/z* = 213; *p*-MeOC₆H₄CH=N-*p*-C₆H₄Cl: *t_r* = 12.554 min, *m/z* = 245; *p*-MeOC₆H₄CH₂NH-*p*-C₆H₄Cl: *t_r* = 12.945 min, *m/z* = 247; *p*-ClC₆H₄CH=N-*p*-C₆H₄OMe: *t_r* = 12.378 min, *m/z* = 245; *p*-ClC₆H₄CH₂NH-*p*-C₆H₄OMe: *t_r* = 12.521 min, *m/z* = 247; *p*-MeOC₆H₄CH=N-*p*-C₆H₄OMe: *t_r* = 13.299 min, *m/z* = 241; *p*-MeOC₆H₄CH₂NH-*p*-C₆H₄OMe: *t_r* = 12.983 min, *m/z* = 243. *p*-FC₆H₄CH=NPh: *t_r* = 8.980 min, *m/z* = 199; *p*-FC₆H₄CH₂NHPh: *t_r* = 9.359 min, *m/z* = 201; PhCH=N-*p*-C₆H₄F: *t_r* = 9.061 min, *m/z* = 199; PhCH₂NH-*p*-C₆H₄F: *t_r* = 9.292 min, *m/z* = 201; Ph(CO)CH₃: *t_r* = 4.573 min, *m/z* = 120; PhCH(OH)CH₃: *t_r* = 4.486 min, *m/z* = 122.

Kinetic Experiments^[4c,29]

Catalytic runs 1–9 (see the Supporting Information, Table S2): In a glove box, a J. Young NMR tube was charged with *N*-benzylideneaniline (according to the required amount from the Supporting Information, Table S1). A freshly prepared stock solution of catalyst **3a** was prepared in [D₈]toluene and an aliquot was added to the *N*-benzylideneaniline. The tube was sealed and removed from the glove box and pressurized with 2 bar H₂. Then, the tube was kept in an oil bath that had been preheated to 140 °C. The typical CH resonance of the *N*-benzylideneaniline (CH=N: singlet, δ = 8.34 ppm) became less intense and the CH₂ signal of the hydrogenated amine product (CH₂-NH: doublet, δ = 4.16 ppm) appeared in the ¹H NMR spectra. The concentrations of the product were determined from integration of the ¹H NMR spectra after an initial 15 min, based on the consumptions of the substrate; the rates are listed in Table S2 in the Supporting Information.

Catalytic runs 10–12 (see the Supporting Information, Table S3): In a glove box, a steel autoclave was charged with *N*-benzylideneaniline (according to the required amount from the Supporting Information, Table S1). A freshly prepared stock solution of catalyst **3a** was prepared

in toluene and an aliquot was added to the *N*-benzylideneaniline. Then, toluene was added to a total volume of 2 mL. The autoclave was closed and removed from the glove box and pressurized with the required H₂ pressure. Then, the autoclave was kept in an oil bath that had been preheated to 140 °C. For each run, three separate experiments were carried out and the conversions were determined at 10, 15, and 20 min intervals by GCMS.

Filtration Experiments

In a 30 mL steel autoclave that was equipped with a stirrer bar, *N*-benzylideneaniline and compound **3b** (5 mg of catalyst **3b** and 165 mg of *N*-benzylideneaniline) were mixed in toluene (0.8 mL). The system was charged with 60 bar H₂ and heated at 140 °C with constant stirring. After 7 min, the reaction was manually terminated by cooling the reaction vessel to RT and removing the maximum amount of H₂ pressure. Then, the autoclave was transferred into a glove box, the rest of the H₂ was released, and the vessel was opened. The solution remained a red color (the same as before the start of the reaction), without the formation of any precipitates or colloids. GCMS analysis revealed approximately 50% conversion. The solution was examined by ³¹P NMR spectroscopy, which indicated the presence of compound **3b**. The solution was filtered through Celite into a new vessel with a new stirrer bar, to which *N*-benzylideneaniline (165 mg) was re-added. No residue was visible on the Celite surface. Then, the catalysis was repeated at 140 °C under 60 bar H₂ and the activity remained the same.

X-ray Diffraction

Single-crystal X-ray diffraction data were collected at 183(2) K on a Xcalibur diffractometer (Agilent Technologies, Ruby CCD detector) for all compounds by using a single-wavelength Enhance X-ray source with MoK_α radiation (λ = 0.71073 Å).^[34a] Suitable single crystals were mounted onto the top of a glass fiber by using polybutene oil and fixed onto a goniometer head that was immediately transferred into the diffractometer. Pre-experiment, data collection, data reduction, and analytical absorption corrections^[34b] were performed with the CrysAlis^{Pro} program suite.^[34a] The crystal structures were solved by using direct methods with SHELXS97.^[34c] The structure refinements were performed by full-matrix least-squares on F² with SHELXL97.^[34c] All of the programs that were used during the crystal-structure determination were included in the WINGX software.^[34d] PLATON^[34e] was used to check the results of the X-ray analysis and DIAMOND^[34f] was used to prepare the molecular graphics.

Acknowledgements

We thank the Swiss National Science Foundation and the University of Zürich for financial support.

- [1] a) J. A. Osborn, F. H. Jardine, J. F. Young, G. Wilkinson, *J. Chem. Soc. A* **1966**, 12, 1711–1732; b) R. R. Schrock, J. A. Osborn, *J. Am. Chem. Soc.* **1976**, 98, 2134–2143; c) C. R. Landis, J. Halpern, *J. Am. Chem. Soc.* **1987**, 109, 1746–1754.
- [2] a) R. Noyori, M. Yamakawa, S. Hashiguchi, *J. Org. Chem.* **2001**, 66, 7931–7944; b) K. J. Haack, S. Hashiguchi, A. Fujii, T. Ikariya, R. Noyori, *Angew. Chem.* **1997**, 109, 297–300; *Angew. Chem. Int. Ed. Engl.* **1997**, 36, 285–288; c) K. Muñiz, *Angew. Chem.* **2005**, 117, 6780–6785; *Angew. Chem. Int. Ed.* **2005**, 44, 6622–6627.
- [3] J. S. M. Samec, J. E. Bäckvall, P. G. Andersson, P. Brandt, *Chem. Soc. Rev.* **2006**, 35, 237.
- [4] a) S. E. Clapham, A. Hadzovic, R. H. Morris, *Coord. Chem. Rev.* **2004**, 248, 2201; b) K. Abdur-Rashid, M. Faatz, A. J. Lough, R. H. Morris, *J. Am. Chem. Soc.* **2001**, 123, 7473–7474; c) K. Abdur-Rashid, S. E. Clapham, A. Hadzovic, J. N. Harvey, A. J. Lough, R. H. Morris, *J. Am. Chem. Soc.* **2002**, 124, 15104–15118; d) H. Berke, *ChemPhysChem* **2010**, 11, 1837–1849.

- [5] a) R. M. Bullock, *Chem. Eur. J.* **2004**, *10*, 2366–2374; b) J. S. Song, D. J. Szalda, R. M. Bullock, C. J. C. Lawrie, M. A. Rodkin, J. R. Norton, *Angew. Chem.* **1992**, *104*, 1280; *Angew. Chem. Int. Ed. Engl.* **1992**, *31*, 1233.
- [6] a) R. Noyori, S. Hashiguchi, *Acc. Chem. Res.* **1997**, *30*, 97–102; b) R. Noyori, T. Okhuma, *Angew. Chem.* **2001**, *113*, 40; *Angew. Chem. Int. Ed.* **2001**, *40*, 40; c) R. Noyori, *Angew. Chem.* **2002**, *114*, 2108–2123; *Angew. Chem. Int. Ed.* **2002**, *41*, 2008–2022; d) M. Yamakawa, H. Ito, R. Noyori, *J. Am. Chem. Soc.* **2000**, *122*, 1466–1478.
- [7] a) M. Ito, T. Ikariya, *Chem. Commun.* **2007**, 5134–5142; b) T. Ikariya, A. J. Blacker, *Acc. Chem. Res.* **2007**, *40*, 1300–1308; c) A. Comas-Vives, G. Ujaque, A. Lledos, *Organometallics* **2007**, *26*, 4135.
- [8] a) J. Zhang, G. Leitus, Y. Ben-David, D. Milstein, *J. Am. Chem. Soc.* **2005**, *127*, 10840–10841; b) J. Zhang, G. Leitus, Y. Ben-David, D. Milstein, *Angew. Chem.* **2006**, *118*, 1131–1133; *Angew. Chem. Int. Ed.* **2006**, *45*, 1113–1115; c) C. Gunanathan, Y. Ben-David, D. Milstein, *Science* **2007**, *317*, 790–792; d) B. Gnanaprakasam, J. Zhang, D. Milstein, *Angew. Chem.* **2010**, *122*, 1510–1513; *Angew. Chem. Int. Ed.* **2010**, *49*, 1468–1471.
- [9] a) Y. Shvo, D. Czarkie, Y. Rahamim, D. F. Chodosh, *J. Am. Chem. Soc.* **1986**, *108*, 7400; b) C. P. Casey, N. A. Strotman, S. E. Beetner, J. B. Johnson, D. C. Priebe, T. E. Vos, B. Khodavandi, I. A. Guzei, *Organometallics* **2006**, *25*, 1230; c) C. P. Casey, H. R. Guan, *J. Am. Chem. Soc.* **2007**, *129*, 5816; d) Y. Blum, D. Czarkie, Y. Rahamim, Y. Shvo, *Organometallics* **1985**, *4*, 1459–1461.
- [10] a) X. Chen, W. Jia, R. Guo, T. W. Graham, M. A. Gullons, K. A. Rashid, *Dalton Trans.* **2009**, 1407–1410.
- [11] a) Z. E. Clarke, P. T. Maragh, T. P. Dasgupta, D. G. Gusev, A. J. Lough, K. A. Rashid, *Organometallics* **2006**, *25*, 4113–4117; b) A. Choualeb, A. J. Lough, D. G. Gusev, *Organometallics* **2007**, *26*, 3509–3515.
- [12] a) M. Bertoli, A. Choualeb, A. J. Lough, B. Moore, D. Spasyuk, D. G. Gusev, *Organometallics* **2011**, *30*, 3479–3482; b) M. Bertoli, A. Choualeb, D. G. Gusev, A. J. Lough, Q. Major, B. Moore, *Dalton Trans.* **2011**, *40*, 8941–8949.
- [13] M. Käß, A. Friedrich, M. Drees, S. Schneider, *Angew. Chem. Int. Ed. Angew. Chem. Int. Ed.* **2009**, *48*, 905–907.
- [14] a) X. F. Wu, D. Vinci, T. Ikariya, J. L. Xiao, *Chem. Commun.* **2005**, 4447; b) K. Murata, T. Ikariya, *J. Org. Chem.* **1999**, *64*, 2186; c) X. Wu, J. Liu, X. Li, A. Zanotti-Gerosa, F. Hancock, D. Vinci, J. Ruan, J. Xiao, *Angew. Chem.* **2006**, *118*, 6870; *Angew. Chem. Int. Ed.* **2006**, *45*, 6718; d) P. Maire, T. Büttner, F. Breher, P. Le Floch, H. Grützmacher, *Angew. Chem.* **2005**, *117*, 6477–6481; *Angew. Chem. Int. Ed.* **2005**, *44*, 6318–6323; e) S. Schneider, J. Meiners, B. Askevold, *Eur. J. Inorg. Chem.* **2012**, 412–419.
- [15] a) R. M. Bullock, *Handbook of Homogeneous Hydrogenation*, Wiley-VCH, Weinheim, **2007**; b) R. M. Bullock, *Catalysis without precious metals*, Wiley-VCH, Weinheim, **2010**.
- [16] a) R. M. Bullock, *Angew. Chem.* **2007**, *119*, 7504–7507; *Angew. Chem. Int. Ed.* **2007**, *46*, 7360–7363; b) K. Junge, K. Schröder, M. Beller, *Chem. Commun.* **2011**, *47*, 4849–4859; c) C. P. Casey, H. Guan, *J. Am. Chem. Soc.* **2009**, *131*, 2499–2507; d) R. Langer, G. Leitus, Y. Ben-David, D. Milstein, *Angew. Chem.* **2011**, *123*, 2168–2172; *Angew. Chem. Int. Ed.* **2011**, *50*, 2120–2124; e) C. Sui-Seng, F. Freutel, A. J. Lough, R. H. Morris, *Angew. Chem.* **2008**, *120*, 954–957; *Angew. Chem. Int. Ed.* **2008**, *47*, 940–943; f) P. O. Lagaditis, A. J. Lough, R. H. Morris, *J. Am. Chem. Soc.* **2011**, *133*, 9662–9665.
- [17] a) R. M. Bullock, M. H. Voges, *J. Am. Chem. Soc.* **2000**, *122*, 12594–12595; b) M. H. Voges, R. M. Bullock, *Dalton Trans.* **2002**, 759–770; c) R. M. Bullock, J. S. Song, *J. Am. Chem. Soc.* **1994**, *116*, 8602–8612; d) B. F. M. Kimmich, P. J. Fagan, E. Hauptman, W. J. Marshall, R. M. Bullock, *Organometallics* **2005**, *24*, 6220–6229; e) V. K. Dioumaev, R. M. Bullock, *Nature* **2000**, *424*, 530–532.
- [18] A. Dybov, O. Blacque, H. Berke, *Eur. J. Inorg. Chem.* **2011**, 652–659.
- [19] a) Y. Jiang, J. Hess, T. Fox, H. Berke, *J. Am. Chem. Soc.* **2010**, *132*, 18233–18247; b) B. Dudle, K. Rajesh, O. Blacque, H. Berke, *J. Am. Chem. Soc.* **2011**, *133*, 8168–8178; c) A. Choualeb, E. Maccaroni, O. Blacque, H. W. Schmalle, H. Berke, *Organometallics* **2008**, *27*, 3474–3481.
- [20] a) S. Chakraborty, O. Blacque, T. Fox, H. Berke, *ACS Catal.* **2013**, *3*, 2208–2217; b) H. Dong, H. Berke, *Adv. Synth. Catal.* **2009**, *351*, 1783–1788.
- [21] Y. Jiang, O. Blacque, T. Fox, C. M. Frech, H. Berke, *Chem. Eur. J.* **2009**, *15*, 2121–2128.
- [22] Y. Jiang, O. Blacque, T. Fox, C. M. Frech, H. Berke, *Organometallics* **2009**, *28*, 5493–5504.
- [23] a) D. Morales, J. Pérez, L. Riera, V. Riera, D. Miguel, M. E. G. Mosquera, S. G. Granda, *Chem. Eur. J.* **2003**, *9*, 4132; b) J. L. Caldarelli, P. S. White, J. L. Templeton, *J. Am. Chem. Soc.* **1992**, *114*, 10097–10103; c) P. Legzdins, S. J. Rettig, K. J. Ross, *Organometallics* **1993**, *12*, 2103–2110; d) K. R. Powell, P. J. Pérez, L. Luan, S. G. Feng, P. S. White, M. Brookhart, J. L. Templeton, *Organometallics* **1994**, *13*, 1851–1864; e) L. W. Francisco, P. S. White, J. L. Templeton, *Organometallics* **1996**, *15*, 5127–5136; f) D. J. Darensbourg, J. D. Draper, B. J. Frost, J. H. Reibenspies, *Inorg. Chem.* **1999**, *38*, 4705–4714.
- [24] a) J. T. Poulton, K. Foltz, W. E. Streib, K. G. Caulton, *Inorg. Chem.* **1992**, *31*, 3190–3191; b) J. T. Poulton, M. P. Sigalas, K. Foltz, W. E. Streib, O. Eisenstein, K. G. Caulton, *Inorg. Chem.* **1994**, *33*, 1476–1485; c) A. Kovacs, G. Frenking, *Organometallics* **2001**, *20*, 2510; d) T. C. Flood, J. K. Lim, M. A. Deming, W. Keung, *Organometallics* **2000**, *19*, 1166; e) S. A. Macgregor, D. MacQueen, *Inorg. Chem.* **1999**, *38*, 4868; f) J. D. Atwood, T. L. Brown, *J. Am. Chem. Soc.* **1976**, *98*, 3160; g) M. Ogasawara, D. Huang, W. E. Streib, J. C. Huffman, N. Gallego-Panas, F. Maseras, O. Eisenstein, K. G. Caulton, *J. Am. Chem. Soc.* **1997**, *119*, 8642–8651.
- [25] a) Z. Chen, H. W. Schmalle, T. Fox, H. Berke, *Dalton Trans.* **2005**, 580–587; b) J. Höck, H. Jacobsen, H. W. Schmalle, G. R. J. Artus, T. Fox, J. I. Amor, F. Bähr, H. Berke, *Organometallics* **2001**, *20*, 1533–1544; c) F. Furno, T. Fox, H. W. Schmalle, H. Berke, *Organometallics* **2000**, *19*, 3620–3630.
- [26] Y. Jiang, B. Schirmer, O. Blacque, T. Fox, S. Grimme, H. Berke, *J. Am. Chem. Soc.* **2013**, *135*, 4088–4102.
- [27] a) L. P. Hammett, *J. Am. Chem. Soc.* **1937**, *59*, 96–103; b) L. P. Hammett, *Chem. Rev.* **1935**, *17*, 125–136; c) X. Yang, L. Zhao, T. Fox, Z.-X. Wang, H. Berke, *Angew. Chem.* **2010**, *122*, 2102; *Angew. Chem. Int. Ed.* **2010**, *49*, 2058.
- [28] a) H. Guan, M. Iimura, M. P. Magee, J. R. Norton, G. Zhu, *J. Am. Chem. Soc.* **2005**, *127*, 7805–7814.
- [29] R. Abbel, K. Abdur-Rashid, M. Faatz, A. Hadzovic, A. J. Lough, R. H. Morris, *J. Am. Chem. Soc.* **2005**, *127*, 1870–1882.
- [30] J. A. Widegren, R. G. Finke, *J. Mol. Catal. A* **2003**, *198*, 317.
- [31] H. Berke, Y. Jiang, X. Yang, C. Jiang, S. Chakraborty, A. Landwehr, *Top. Curr. Chem.* **2013**, *334*, 27–57.
- [32] a) K. Seyferth, R. Taube, *J. Organomet. Chem.* **1982**, *229*, 275–279; b) A. A. Danopoulos, A. R. Wills, P. G. Edwards, *Polyhedron* **1990**, *9*, 2413–2418.
- [33] CCDC 888511 (**1a**), CCDC 888512 (**1b**), CCDC 888513 (**2a**), CCDC 888514 (**3a**), and CCDC 888515 (**3b**) contain the supplementary crystallographic data for this paper. These data can be obtained free of charge from The Cambridge Crystallographic Data Centre via www.ccdc.cam.ac.uk/data_request/cif.
- [34] a) Agilent Technologies (formerly Oxford Diffraction), Yarnton, England, **2011**; b) R. C. Clark, J. S. Reid, *Acta Crystallogr. Sect. A* **1995**, *51*, 887–897; c) G. M. Sheldrick, *Acta Crystallogr. Sect. A* **2008**, *64*, 112–122; d) L. J. Farrugia, *J. Appl. Crystallogr.* **1999**, *32*, 837; e) A. L. Spek, *J. Appl. Crystallogr.* **2003**, *36*, 7–13; f) K. Brandenburg, *DIAMOND*, Crystal Impact GbR, Bonn, **2007**.

Received: August 16, 2013

Published online: October 15, 2013